Journal of Statistical Physics, Vol. 83, Nos. 1/2, 1996

Hard Chaos and Adiabatic Quantization: The Wedge Billiard

T. Szeredi[1]

Received December 1, 1994; final April 20, 1995

We present a study of a series of eigenstates occurring in the wedge billiard which may be quantized about tori by semiclassical adiabatic quantization, even though the underlying classical system exhibits hard chaos and strictly possesses no tori. We also show that adiabatic eigenstates should be common in many chaotic systems, especially among the lower eigenstates, and present a heuristic argument as to why this should be so.

KEY WORDS: Classical chaos; quantum chaos; adiabatic; quantization; Born–Oppenheimer; wedge; billiard; hard chaos; semiclassical.

1. INTRODUCTION

In this paper we examine the relationship between a classical system showing hard chaos and its quantum counterpart via adiabatic semiclassical quantization,[1] also known as Born–Oppenheimer quantization.[2] Semiclassical methods are useful because it is in the semiclassical regime where we may attempt to apply our classical intuition to the often nonintuitive results of quantum mechanics; we can try to 'make sense' of the quantum results. We use classical adiabatic methods[8] coupled with the uncertainty principle to understand a certain class of eigenstates, which we call *adiabatic eigenstates*, seen in the quantum analog of a classical system showing hard chaos.

The surprising fact is that the quantum system behaves as though it 'sees' an integrable classical system for these eigenstates and quantizes eigenstates around nonexistent classical tori. The quantum eigenfunctions

[1] Department of Applied Mathematics, The Open University, Milton Keynes, MK7 6AA, United Kingdom.

0022-4715/96/0400-0259$09.50/0

are 'scarred' by classical structures which, strictly speaking, only exist for finite time scales.

We believe that such adiabatic eigenstates are ubiquitous in many systems showing hard chaos. The hyperbola billiard[3] with its adiabatic horn eigenstates[1] and the stadium billiard[4] with its whispering gallery adiabatic eigenstates[2] are just two examples of such adiabatic eigenstates occurring in billiard systems. They also occur in smooth potentials which show chaos, such as the quartic oscillator[5] and nonhydrogenic atoms in magnetic fields.[6] The fraction of eigenstates which are adiabatic eigenstates relative to the total number of eigenstates is significant, especially for the low-lying levels which are often the basis of numerical and experimental investigations. Given the ubiquity of these adiabatic eigenstates and their significant numbers, it is essential to have a clear, intuitive understanding of them if we are to understand the correspondence between classical and quantal chaos.

The plan of this paper is as follows. In Section 2 we briefly review the relevant ideas of classical and quantal adiabatic theory. We introduce the wedge billiard and apply the ideas of adiabatic quantization to the wedge billiard and obtain the semiclassical eigenvalues of the adiabatic eigenstates. We show that the number of such adiabatic eigenstates, as a fraction of the total number of eigenstates, is quite significant. The adiabatic eigenstates typically constitute about 10% of the first 100 eigenstates. Furthermore, this fraction only decreases slowly with energy. In Section 3 we introduce the notion of quantum and classical Wigner functions for the wedge billiard. In Section 4 we present the results of numerical calculations of the eigenvalues and eigenfunctions of the wedge billiard and show a series of scarred adiabatic eigenstates. We compare the adiabatic predictions with the numerical results and find excellent agreement. In Section 5 we discuss the results and propose further avenues for exploration and research.

2. CLASSICAL AND QUANTAL ADIABATIC THEORY: THE WEDGE BILLIARD

We briefly review the classical theory of adiabatic invariance.[8] Consider the one-dimensional Hamiltonian

$$H = H(q, p, \lambda) \tag{1}$$

Here we consider λ a parameter. We assume that, for λ constant, there exist action–angle variables for the system for some range of parameter values $\lambda_1 \leqslant \lambda \leqslant \lambda_2$.

The action, which is defined by

$$J = \frac{1}{2\pi} \oint_{\mathcal{C}} p(q, H, \lambda)\, dq \tag{2}$$

is then also a constant of the motion.

The classical theory of adiabatic invariance states that if we now allow λ to vary slowly with time, then J as defined in Eq. (2) is still an approximate constant of the motion.

The connection with quantum mechanics is made by the usual EBK semiclassical quantization rule,[9] which states that the classical action must be quantized according to

$$J = (n + u/4)\hbar, \qquad n = 0, 1, 2,... \tag{3}$$

where u is a positive integer, called the Maslov index, which characterizes the number of times the semiclassical approximation breaks down along the traversal of a cycle in evaluating the integral in Eq. (2).

We now proceed to apply these ideas to the specific system we are studying. The classical system is known as the wedge billiard, and has been the subject of previous classical[10] and quantal[11] investigations. The wedge billiard consists of a particle of mass m confined to the region between the Y axis and the line $Y = X \cot \phi$, ϕ being the wedge angle. We

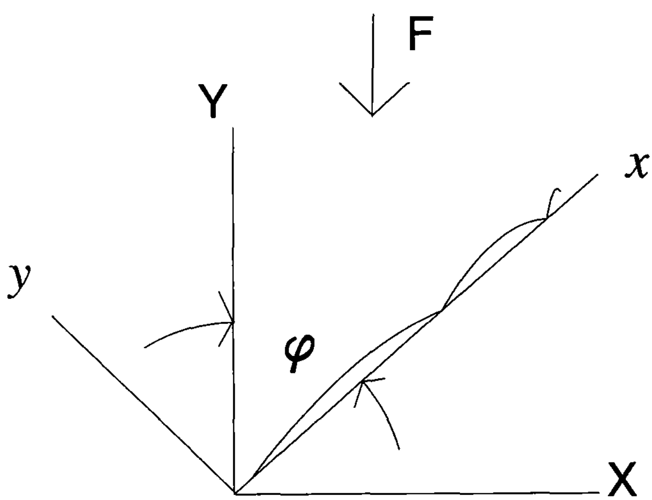

Fig. 1. The geometry of the wedge billiard. The relationship between the two sets of coordinates [the usual (X, Y) coordinates, and the (x, y) coordinates which point along the tilted wall and perpendicular to the tilted wall, respectively] is shown. Also shown is part of a typical glancing trajectory where the particle makes several shallow bounces along the tilted wall.

assume the particle makes elastic collisions with the wedge boundaries and is acted upon by a constant force F in the negative Y direction as in Fig. 1. The Hamiltonian is

$$H = \frac{1}{2m}(p_X^2 + p_Y^2) + FY, \qquad X \geqslant 0, \quad Y \geqslant X \cot \phi \tag{4}$$

where p_X and p_Y are the momenta in the X and Y directions, respectively.

For wedge angles less than 45° the system exhibits soft chaos; the phase space consists of regions of chaos interspersed with invariant tori. For $\phi = 45°$ the system is integrable; the phase space is entirely filled with invariant tori. For wedge angles between 45° and 90° the system exhibits hard chaos;[10] there are no invariant tori in the phase space and all periodic orbits are unstable.

We change coordinates to those coordinates, (x, y), which run parallel (x), and perpendicular (y) to the tilted wall of the wedge, as in Fig. 1. In this way we isolate the 'fast' from the 'slow' motion:

$$x = X \sin \phi + Y \cos \phi, \qquad y = -X \cos \phi + Y \sin \phi \tag{5}$$

Then, in the new variables the Hamiltonian is

$$H = \frac{p_x^2}{2m} + Fx \cos \phi + \frac{p_y^2}{2m} + Fy \sin \phi, \qquad 0 \leqslant y \leqslant x \tan \phi \tag{6}$$

Consider the motion of the particle on those classical trajectories where the particle glances at a very shallow angle along the tilted wall. This is a very special subset of all possible motions in phase space. However, it turns out to have profound consequences on the quantum system. During this motion the frequency of the motion in the y direction is much greater than that in the x direction. This means that during one bounce in the y direction x may be treated as approximately constant. We write Eq. (6) as

$$H = \frac{p_x^2}{2m} + H_y(x) \tag{7}$$

where

$$H_y(x) = \frac{p_y^2}{2m} + Fx \cos \phi + Fy \sin \phi \tag{8}$$

In the Hamiltonian $H_y(x)$, x may be regarded as a slowly varying parameter; the principle of adiabatic invariance may be used. The action in the y variable, J_y, is an approximate constant of the motion,

$$
\begin{aligned}
J_y &= \frac{1}{2\pi} \oint_C p_y(x, E_y)\, dy \\
&= 2\,\frac{1}{2\pi} \int_0^{E_y/(F\sin\phi) - x/\tan\phi} \{2m[(E_y - Fx\cos\phi) - Fy\sin\phi]\}^{1/2}\, dy \\
&= \frac{2(2m)^{1/2}}{3\pi F\sin\phi} (E_y - Fx\cos\phi)^{3/2} \qquad (9)
\end{aligned}
$$

or solving for E_y we get

$$E_y = \left(\frac{3\pi F\sin\phi}{2(2m)^{1/2}} J_y\right)^{2/3} + Fx\cos\phi \qquad (10)$$

Since J_y is approximately constant during the x motion up and down the tilted wall, we may use Eq. (10) in Eq. (7) to get our adiabatic Hamiltonian in x as

$$H_{\mathrm{ad}}(x) = \frac{p_x^2}{2m} + Fx\cos\phi + \left(\frac{3\pi F\sin\phi}{2(2m)^{1/2}} J_y\right)^{2/3} \qquad (11)$$

The action variable for the x motion is found in an exactly analogous manner, giving

$$J_x = \frac{2(2m)^{1/2}}{3\pi F\cos\phi}\left[E - \left(\frac{3\pi F\sin\phi}{2(2m)^{1/2}} J_y\right)^{2/3}\right]^{3/2} \qquad (12)$$

Equation (12) can be solved for E to give

$$E = \left(\frac{3\pi F\cos\phi}{2(2m)^{1/2}} J_x\right)^{2/3} + \left(\frac{3\pi F\sin\phi}{2(2m)^{1/2}} J_y\right)^{2/3} \qquad (13)$$

Since J_x and J_y are separately conserved during the glancing clasical motion and since the Hamiltonian is an additive function of x and y separately, it is now tempting to set equal the corresponding pieces in Eqs. (6) and (13) to get

$$\frac{p_x^2}{2m} + Fx\cos\phi \approx \left(\frac{3\pi F\cos\phi}{2(2m)^{1/2}} J_x\right)^{2/3} \qquad (14)$$

$$\frac{p_y^2}{2m} + Fy\sin\phi \approx \left(\frac{3\pi F\sin\phi}{2(2m)^{1/2}} J_y\right)^{2/3} \qquad (15)$$

This classical adiabatic theory remains valid for the glancing motion up and down the tilted wall as long as the frequency of motion in the y

direction, ω_y, is much greater than that in the x direction, ω_x. The classical frequencies are defined by

$$\omega_x = \frac{\partial E(J_x, J_y)}{\partial J_x}, \qquad \omega_y = \frac{\partial E(J_x, J_y)}{\partial J_y} \tag{16}$$

Upon using Eq. (13) in Eq. (16) and the validity criterion of the adiabatic theory, $\omega_y \gg \omega_x$, we arrive at

$$J_x \tan^2 \phi \gg J_y \tag{17}$$

Semiclassically we have the EBK quantization rule[9]

$$J_k = \hbar(n_k + u_k/4), \qquad k = x, y \tag{18}$$

For billiards the Maslov index u_k must be incremented by two at each hard-wall collision. For both the x and y motions we have one semiclassical breakdown at the upper turning point and one hard-wall collision per cycle, which gives $u_k = 3$.

Using the semiclassical quantization rule (18) in Eq. (13) gives us our semiclassical adiabatic eigenvalues

$$E_{n_x, n_y} = \left(\frac{3\pi\hbar F}{2(2m)^{1/2}}\right)^{2/3} \left\{\left[\left(n_x + \frac{3}{4}\right)\cos\phi\right]^{2/3} + \left[\left(n_y + \frac{3}{4}\right)\sin\phi\right]^{2/3}\right\} \tag{19}$$

The condition for the validity of the adiabatic approximation, Eq. (17), may be cast in a quantum form using Eq. (18) to give us the result that in the quantum system we must have

$$n_x \tan^2 \phi \gg n_y \tag{20}$$

for the quantum adiabatic approximation to be valid.

How many states, as a fraction of the total number of states at some energy, can we expect to be quantized in such an adiabatic fashion? Because of the restriction from Eq. (20) that $n_x \gg n_y$ we essentially have a one-dimensional problem where n_y remains small and constant, and n_x varies. Then, differentiating Eq. (19) with respect to n_x, we have that

$$\frac{\partial E}{\partial n_x} = \frac{2}{3}\left(\frac{3\pi\hbar F \cos\phi}{2(2m)^{1/2}}\right)^{2/3} \frac{1}{(n_x + 3/4)^{1/3}} \tag{21}$$

and using the fact that, for large n_x (and hence large E), we have from Eq. (19)

$$\left(n_x + \frac{3}{4}\right) \approx \left(\frac{2(2m)^{1/2}}{3\pi\hbar F}\right)^{1/2} E^{3/2} \tag{22}$$

we find

$$dn_x \approx \frac{(2m)^{1/2} E^{1/2} \, dE}{\pi \hbar F \cos \phi} \tag{23}$$

For the full two-dimensional problem[11] the density of states for the wedge billiard is

$$\frac{dN}{dE} \approx \frac{mE^2}{4\pi \hbar^2 F^2 \cot \phi} \tag{24}$$

where N is the total number of states below energy E. Upon using Eqs. (23) and (24) we find that

$$\frac{dn_x}{dN} \approx 4 \left(\frac{2}{m}\right)^{1/2} \frac{F\hbar}{\sin \phi} \frac{1}{E^{3/2}} \approx 4[\pi \sin(2\phi)]^{1/2} \frac{1}{N^{1/2}} \tag{25}$$

One sees that although $\lim_{N \to \infty} dn_x/dN = 0$, the approach to this limit is quite slow. In particular, for the lower eigenstates, where, say, $N \leqslant 100$, we find that a substantial fraction of them (of order 10% or more) are adiabatic eigenstates.

Do adiabatic states make up a significant fraction of states in other systems as well? Consider a finite-area, free-particle, concave billiard, such as the integrable circle billiard[11] or the chaotic stadium billiard.[4] For such billiards[12]

$$N = \frac{mAE}{2\pi \hbar^2} \tag{26}$$

where A is the area of the billiard. Supposing that the classical particle exhibits adiabatic motion around the boundary, such as the whispering gallery eigenstates in the stadium, this motion may be adiabatically quantized to give[2]

$$E \approx \frac{\hbar^2 \pi^2}{2mL^2} n^2 \tag{27}$$

where L is the perimeter of the billiard and n is a quantum number for motion along the boundary and we assume that the adiabatic quantum number for motion perpendicular to the boundary is much smaller than n. Then the fraction of eigenstates which are adiabatic is given by

$$\frac{dn}{dN} = \frac{L}{\pi A^{1/2}} \frac{1}{N^{1/2}} \tag{28}$$

In general, for leading-order behavior of $N(E)$ and $n(E)$ given by

$$N(E) \propto E^{\gamma}, \qquad n(E) \propto E^{\beta} \tag{29}$$

where $\beta \leqslant \gamma$, then

$$\frac{dn}{dN} \propto N^{(\beta/\gamma - 1)} \tag{30}$$

Thus, even in the scenario of $\gamma \to \infty$, the fraction of eigenstates which are adiabatic should fall off as $1/N$, which is not a very small number.

For the hyperbola billiard[3,1] $N \approx E \ln E/2\pi$ and $E \approx \pi(n_x + 1)(n_y + 1)/2$. Again keeping n_y constant, we get

$$dN \approx \frac{n_y + 1}{4} \ln\left(\frac{\pi n_x}{2}\right) dn_x \tag{31}$$

Indeed, in this system the adiabatic eigenstates constitute an almost constant fraction of eigenstates in the large-N limit.

These theoretical calculations are borne out by numerical studies of chaotic quantum systems[1,4–7] which confirm that adiabatic eigenstates are common in chaotic systems, especially among the lower eigenstates.

There is a somewhat heuristic, but nonetheless appealing argument as to why adiabatic eigenstates are common among the lower eigenstates. If one considers the simple semiclassical quantization criterion $\Delta E \, \Delta T \approx h$, then as long as the spacing between eigenvalues ΔE is large, classical motions with relatively short periods (small ΔT) have a chance at quantizing the motion. The fact that the classical motion over long time scales is chaotic is not important for the low-lying eigenstates (with large ΔE); all that matters is motion on 'short' time scales. Hence the fact that the particle eventually completes its glancing motion up and down the tilted wall of the wedge billiard does not matter. What matters is that for a short time the particle behaves as if it was on a torus of an integrable system and this is what the quantum mechanics 'sees.' As one goes higher in the eigenspectrum the density of states increases and hence ΔE decreases. Thus, the classical particle must stay on a classical structure for longer and longer times for the quantum mechanics to 'see' the classical structure. Correspondingly less of the classical phase space contains such approximately conserved structures[13] and so the fraction of adiabatic states diminishes, and since the classical system is actually chaotic and ergodic, goes to zero with increasing energy.

3. WIGNER FUNCTIONS

One could also carry through the adiabatic quantization procedure on the eigenfunctions and arrive at semiclassical, adiabatic eigenfunctions in coordinate space. However, since the spirit of adiabatic quantization lies with quantizing structures in phase space, the Wigner function[14–16] of an eigenstate is a more appropriate object to study.

The eigenstate Wigner function for an eigenstate of the wedge billiard with energy E_n is defined by

$$\begin{aligned}\mathscr{W}&(x, y, p_x, p_y; E_n)\\ &=\frac{1}{(\pi\hbar)^2}\int_{-\infty}^{\infty} d\xi_1 \int_{-\infty}^{\infty} d\xi_2 \exp\left(-\frac{2i}{\hbar}(p_x\xi_1 + p_y\xi_2)\right)\\ &\quad\times \psi_n^*(x+\xi_1, y+\xi_2)\,\psi_n(x-\xi_1, y-\xi_2)\end{aligned} \tag{32}$$

where $\psi_n(x, y)$ is the quantum eigenfunction, which is a solution to the eigenvalue equation obtained from substituting operators into Eq. (6), namely

$$\left\{\frac{-\hbar^2}{2m}\left(\frac{\partial^2}{\partial x^2}+\frac{\partial^2}{\partial y^2}\right)+F(x\cos\phi + y\sin\phi)\right\}\psi_n(x, y) = E_n\psi_n(x, y) \tag{33}$$

The boundary conditions for Eq. (33) are $\psi_n(x, 0) = 0$ and $\psi_n(x, x\tan\phi) = 0$.

Classical particles are described in quantum mechanics by wave packets, which are sums over eigenstates. In phase space, the analog of a classical particle with energy near E_N is a sum over eigenstate Wigner functions centered on the classical energy. We define such sums over Wigner functions by

$$\bar{\mathscr{W}}(x, y, p_x; E_N) = \sum_n a(n)\,\mathscr{W}(x, y, p_x; E_n) \tag{34}$$

where $a(n)$ is some function strongly peaked about the energy of the classical particle, E_N. For example, to describe quantum mechanically a semiclassical* microcanonical ensemble centered around E_N one could choose $a(n) = 1/(N_{max} - N_{min})$ if $N_{min} < n < N_{max}$, $N = (N_{max} - N_{min})/2$, $N \gg N_{max} - N_{min} \gg 1$, and $a(n) = 0$ otherwise. The condition $N \gg 1$ ensures that the system is semiclassical; the combined condition $N \gg N_{max} - N_{min} \gg 1$ ensures that the members of the ensemble have approximately the same energy and that the slab in energy space is classically 'thin' yet quantum mechanically 'thick.' Hence the quantum ensemble mimics a classical microcanonical ensemble. On the other hand, the eigenstate Wigner function for an eigenstate labeled by N is given by setting $a(n)=\delta_{N,n}$ in Eq. (34).

The beauty of the Wigner function (34) is that in the classical limit of $\hbar \to 0$ (which in this case is given by $N \gg 1$) different behaviors are expected for ergodic and integrable systems.[15,16] For an ergodic, classically chaotic system the limiting form of its Wigner function, which we will call the classical Wigner function, is

$$\lim_{\hbar \to 0} \bar{\mathscr{W}}(\mathbf{q}, \mathbf{p}; E_N) \approx \frac{\delta[E_N - H(\mathbf{q}, \mathbf{p})]}{\int \cdots \int d\mathbf{q}\, d\mathbf{p}\, \delta[E_N - H(\mathbf{q}, \mathbf{p})]} \tag{35}$$

whereas for an integrable classical system

$$\lim_{\hbar \to 0} \bar{\mathscr{W}}(\mathbf{q}, \mathbf{p}; E_N) \approx \frac{1}{(2\pi)^D} \delta[\mathbf{J}(\mathbf{q}, \mathbf{p}) - \mathbf{J}_N] \tag{36}$$

where $H(\mathbf{q}, \mathbf{p})$ is the classical Hamiltonian of the D-dimensional system and $\mathbf{J}(\mathbf{q}, \mathbf{p})$ is the classical action [a constant of the motion, as in Eqs. (14), (15)] and $\mathbf{J}_N$ is the quantized value of this action corresponding to the quantum number N [as in Eq. (18)]. These classical limits of the Wigner functions are none other than the classical phase space densities. In Eq. (35) the classical phase space density is for a classical microcanonical ensemble with energy E_N. In Eq. (36) the classical phase space density is for a microcanonical ensemble with energy E_N and which is further constrained to lie on tori.

In the classical limit, we expect the Wigner function to be one of two types[15,16]: either spread out uniformly over the energy shell [Eq. (35)] if there are no constants of the motion besides the energy, or concentrated on classical tori [Eq. (36)] if there are constants of the motion besides the energy. Since the adiabatic eigenstates have two approximate constants of the motion (the actions in the x and y directions are separately conserved), we expect the Wigner functions constructed from the adiabatic eigenstates to be concentrated on classical tori. In contrast, the Wigner functions constructed from the 'ergodic' quantum eigenstates should be spread out across the energy shell.

In the semiclassical regime the eigenstate Wigner function (32) has a rich structure,[16] with maxima located on the conserved classical quantities, characteristic oscillations as one moves away from the maxima toward the classically accessible region, and an exponential decay as one moves from the maxima toward the classically inaccessible region.

Since the wedge billiard has two spatial dimensions, the Wigner function is four-dimensional. Such four-dimensional objects are difficult to visualize, so we will project out the y component of the Wigner function to leave us with a function of x and p_x as follows; define

$$W(x, p_x; E_N) = \int_0^{\infty} dy \int_{-\infty}^{\infty} dp_y \, \mathscr{W}(x, y, p_x, p_y; E_N) \tag{37}$$

Wigner functions such as Eq. (37) will be the main objects of our study of the adiabatic eigenstates of the wedge billiard.

For the wedge billiard the classical Wigner functions, Eqs. (35) and (36), may be analytically evaluated. We omit the details and here we quote the results. For ergodic behavior we have from Eqs. (35) and (37)

$$\begin{aligned} W(x, p_x; E_N) = \frac{(2m)^{1/2} \cos\phi}{E_N^2 \sin^2\phi} \Bigg\{ & \left[E_N - \left(\frac{p_x^2}{2m} + Fx \cos\phi \right) \right]^{1/2} \\ & - \left[E_N - \left(\frac{p_x^2}{2m} + \frac{Fx}{\cos\phi} \right) \right]^{1/2} \Bigg\} \end{aligned} \tag{38}$$

for $p_x^2/(2m) + Fx/\cos\phi \leqslant E_N$ and

$$W(x, p_x; E_N) = \frac{(2m)^{1/2} \cos\phi}{E_N^2 \sin^2\phi} \left\{ \left[E_N - \left(\frac{p_x^2}{2m} + Fx \cos\phi \right) \right]^{1/2} \right\} \tag{39}$$

for $p_x^2/(2m) + Fx \cos\phi \leqslant E_N < p_x^2/(2m) + Fx/\cos\phi$ and $W(x, p_x; E_N) = 0$ otherwise.

For adiabatic behavior we have from Eqs. (36) and (37) that

$$W(x, p_x; E_N) = \frac{1}{2\pi} \delta[J_x(x, p_x) - J_{N_x}] \tag{40}$$

where $J_x(x, p_x)$ is defined by Eq. (14) and J_{N_x} is defined by Eq. (18).

4. RESULTS

The exact eigenvalues and eigenfunctions for the wedge billiard have previously been calculated by a large matrix diagonalization.[11] For the matrix diagonalization and the figures shown in this paper scaled units[11] have been used; this is equivalent to setting $\hbar = m = F = 1$. Figure 2a shows a plot of a 'regular' eigenfunction, labeled by $N = 57$, which is localized along the tilted wall of the wedge, highly suggestive that this is an adiabatic eigenstate. Figure 2b shows a typical 'irregular' eigenfunction, $N = 56$. By scanning plots of the eigenstates we can pick out a series of localized adiabatic eigenstates, each member having zero nodes in the y direction

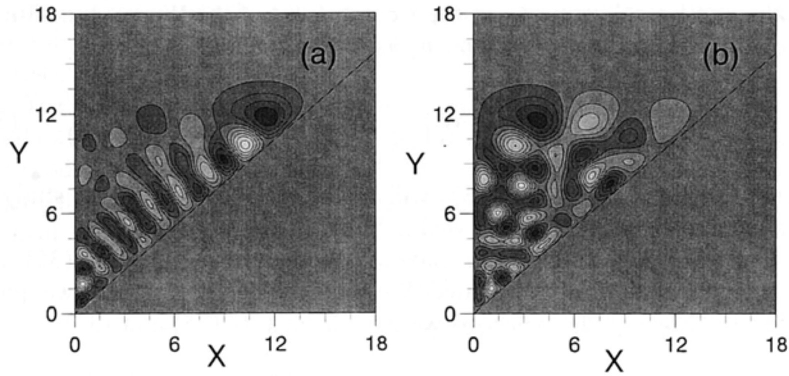

Fig. 2. Shaded contour plots of $\psi(X, Y)$ for (a) an adiabatic eigenstate (labeled by quantum number $N=57$) and (b) a typical 'chaotic' eigenstate (labeled by quantum number $N=56$).

($n_y=0$), and each successive member in the series having another node in the x direction ($n_x=1$, 2, 3,...). These adiabatic eigenstates should be concentrated on the classical tori given by Eq. (40).

Figures 3a and 3b show plots of the corresponding eigenstate Wigner functions, Eq. (37) with $a(n)=\delta_{N,n}$, for eigenstates $N=57$ and $N=56$, respectively. These should be compared with Figs. 4a and 4b, which show the classical Wigner functions, Eq. (40) and Eqs. (38) and (39), respectively, evaluated at the energy of eigenstates $N=57$, 56. It is clear that the adiabatic eigenstate in Fig. 3a is strongly localized near the classical torus shown in Fig. 4a, with characteristic oscillations as one moves into the classically accessible region. The irregular eigenstate in Fig. 3b has much

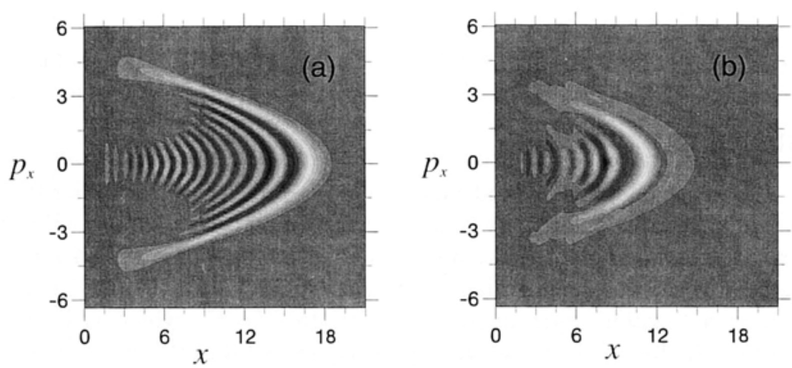

Fig. 3. Shaded plots of the eigenstate Wigner functions (37), with $a(n)=\delta_{N,n}$. The plots correspond to (a) an adiabatic eigenstate (labeled by quantum number $N=57$) and (b) a typical 'chaotic' eigenstate (labeled by quantum number $N=56$).

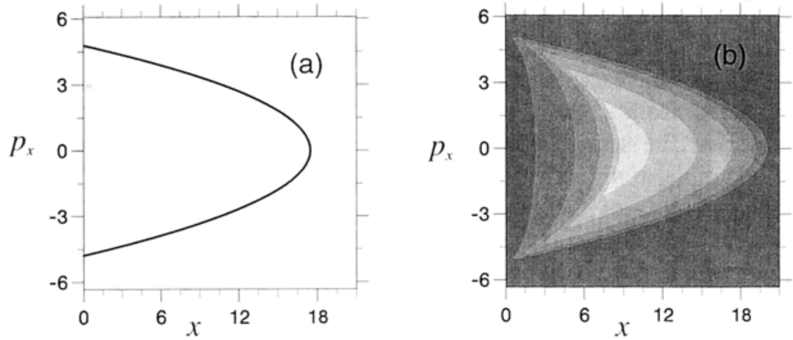

Fig. 4. Plots of the classical Wigner functions corresponding to (a) an adiabatic state, Eq. (40), which is a delta function on the classical torus, and (b) an 'ergodic' state, Eqs. (38) and (39), which is a uniform distribution on the energy shell.

more in common with Fig. 4b than Fig. 4a; it is concentrated more toward the center of the classically allowed region and avoids the torus.

We can get a clearer picture of the classical–quantal correspondence by forming a sum over adiabatic and ergodic eigenstates, respectively, as suggested by the classical ensembles implied in Eqs. (35), (36): Summing the eigenstate Wigner functions for adiabatic eigenstates $N=51$, 57, 63 as in Eq. (34), we generate a quantum microcanonical ensemble which should closely mimic Eq. (36). The results are shown in Fig. 5a. The Wigner function is strongly concentrated on the classical torus shown in Fig. 4a and most of the oscillations in the classically accessible region have been averaged away. Summing the eigenstate Wigner functions for 10 irregular eigenstates $N=52$, 53, 54, 55, 56, 58, 59, 60, 61, 62, we generate a quantum

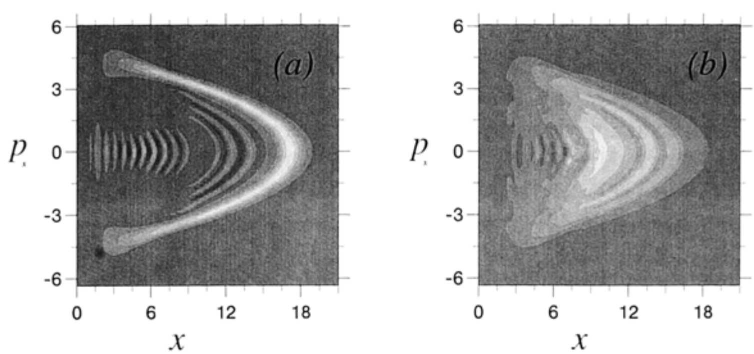

Fig. 5. Shaded plots of Wigner functions (37) corresponding to semiclassical microcanonical ensembles of (a) adiabatic eigenstates (normalized sum over eigenstates labelled by $N=51$, 57, 63) and (b) 'chaotic' eigenstates (normalized sum over 10 eigenstates labeled by $N=52$, 53, 54, 55, 56, 58, 59, 60, 61, 62).

microcanonical ensemble which should closely mimic Eq. (35) corresponding to an ergodic classical situation. The results are shown in Fig. 5b, and are seen to have a close correspondence with Fig. 4b. The ensemble constructed from regular eigenstates is a good example of caustic-type behavior in the semiclassical limit; the irregular eigenstate ensemble is a good example of anticaustic-type behavior.[15,16]

Using plots of the eigenstates and Wigner functions such as Figs. 2 and 3, we are able unambiguously to pick out and label, by a pair of integers (n_x, n_y), the adiabatic eigenstates of the wedge billiard. Using these integers in the adiabatic quantization condition, we obtain from Eq. (19) the adiabatic eigenvalues shown in the second column of Table I. The exact eigenvalues (labeled by N) are shown in column 4, and column 5 shows the difference between the exact eigenvalues and the adiabatic eigenvalues. One sees that the adiabatic eigenvalues are consistently higher, by an almost constant amount, than the exact eigenvalues. This is probably because of the failure of the adiabatic quantization properly to account for the boundary conditions near the wedge vertex. Evidence of this failure can be seen in Figs. 3a and 5a); the Wigner functions do not follow the classical torus

Table I. Comparison Between Adiabatic Eigenvalues and Exact Quantum Eigenvalues for States Identified as $n_y = 0$ Adiabatic States for the 49° Wedge

n_x	E_{n_x,n_y}	N	E_N	$E_N - E_{n_x,n_y}$	$E_{n_x,n_y} + c$
1	3.973	1	3.816	−0.157	3.861
2	4.833	2	4.712	−0.121	4.721
3	5.592	3	5.472	−0.120	5.481
4	6.286	5	6.171	−0.115	6.175
5	6.933	7	6.823	−0.109	6.821
6	7.543	10	7.442	−0.100	7.431
7	8.123	12	8.018	−0.105	8.011
8	8.679	15	8.585	−0.094	8.567
9	9.214	19	9.137	−0.077	9.102
10	9.731	23	9.679	−0.052	9.619
11	10.232	26	10.091	−0.142	10.121
12	10.719	30	10.586	−0.133	10.608
13	11.194	35	11.068	−0.126	11.082
14	11.657	40	11.537	−0.121	11.546
15	12.110	45	11.993	−0.117	11.998
16	12.554	51	12.441	−0.113	12.442
17	12.988	57	12.879	−0.109	12.876
18	13.415	63	13.310	−0.104	13.303
19	13.834	70	13.727	−0.107	13.722

in Fig. 4a right into the vertex at $x=0$. Denoting the average of the difference between the exact and adiabatic eigenvalues listed in the table by

$$c=\overline{(E_N-E_{n_x,n_y})}=-0.112$$

we list the modified adiabatic eigenvalues, $E_{n_x,n_y}+c$, in column 6. The agreement between the exact eigenvalues and the modified adiabatic eigenvalues is excellent.

5. DISCUSSION

We have shown how adiabatic quantization can provide a qualitative and quantitative understanding of a series of adiabatic eigenstates in the wedge billiard. By plotting the Wigner functions of these states we can clearly see the scarring of the adiabatic eigenstates by the classical tori in phase space. The somewhat surprising point is that the classical motion of all trajectores (except a set of zero measure) is ergodic and chaotic, and hence, strictly speaking, there are no tori in the classical phase space. Only when one looks on 'short' time scales (defined by the mean level spacing and $\Delta E\,\Delta T\approx\hbar$) does the quantum system 'see' a classical torus which can be quantized.

We have also shown that these adiabatic eigenstates can be expected in relatively large numbers, especially at low energies, in chaotic systems, even those classically showing hard chaos. Hence, they must play an important role in calculations and experiments with chaotic systems.

Several unanswered and partly open questions remain about the role of these adiabatic states in quantum chaos. The adiabatic states are localized about classical invariant tori and hence are not ergodic. Yet, the classical system is ergodic and chaotic; at what stage (in increasing N) can one reasonably expect a wave packet to display ergodic behavior? Can special wave packets be constructed which will show localization on tori even for very large N? Will the memory of the adiabatic states persist up to the classical limit?

The fact that there is a regular component to the spectrum also introduces the possibility of deviations from GOE[17] statistics in the level spacings. It can be anticipated that there are many approximate adiabatic constants in chaotic systems, each one producing a regular spectrum and deviations from GOE. How far into the classical limit must one go to see these deviations disappear?

One of the most illuminating and successful approaches to the study of quantum chaos in recent years has been the periodic orbit approach.[17]

Some work[1,5] has been done on the connections between adiabatic quantization and periodic orbit theory; however, the exact way in which periodic orbits contribute to the adiabatic eigenvalues is still far from clear. This connection is particularly important because the point at which adiabatic quantization appears to work, namely for classical motion almost confined to classical tori, is the point at which the periodic orbit theory has the most trouble.[11,1]

ACKNOWLEDGMENTS

I would like to thank SERC (in Great Britain) and NSERC (in Canada) for financial support of this work.

REFERENCES

1. P. Dahlqvist, *J. Phys. A* **25**:6265 (1992).
2. Y. Y. Bai, B. Hose, K. Stefanski, and H. S. Taylor, *Phys. Rev. A* **31**:2821 (1985).
3. M. Sieber and F. Steiner, *Physica D* **44**:248 (1990).
4. S. W. McDonald, Ph.D. Thesis, University of California (Berkeley) (1983).
5. B. Eckhardt, G. Hose, and E. Pollak, *Phys. Rev. A* **39**:3776 (1989).
6. P. A. Dando, T. S. Montiero, W. Jans, and W. Schwiezer, *Prog. Theor. Phys. Suppl.* **116**:403 (1994).
7. W. Jans, T. S. Montiero, W. Schweizer, and P. A. Dando, *J. Phys. A* **26**:3187 (1993).
8. I. C. Percival and D. Richards, *Introduction to Dynamics* (Cambridge University Press, Cambridge, 1982).
9. L. I. Schiff, *Quantum Mechanics*, 3rd ed. (McGraw-Hill, New York, 1968); S. K. Knudson and D. W. Noid, *J. Chem. Ed.* **66**:133 (1989).
10. T. Szeredi and D. A. Goodings, *Phys. Rev. E* **48**:3518 (1993); N. D. Whelan, D. A. Goodings, and J. K. Cannizzo, *Phys. Rev. A* **42**:742 (1990); N. I. Chernov, *Physica D* **53**:233 (1991); M. P. Wojtkowski, *Commun. Math. Phys.* **126**:507 (1990); P. H. Richter, H. J. Scholz, and A. Wittek, *Nonlinearity* **3**:45 (1990); H. E. Lehtihet and B. N. Miller, *Physica D* **21**:93 (1986).
11. T. Szeredi, J. H. Lefebre, and D. A. Goodings, *Nonlinearity* **7**:1463 (1994); T. Szeredi and D. A. Goodings, *Phys. Rev. E* **48**:3529 (1993); C. Rouvinez and U. Smilansky, *J. Phys. A* **28**:77 (1995); A. Wittek, Die Quantenmechanik eines nichtintegrablen systems; klassisch chaotisches billiard in gravitationsfeld, Ph.D. Thesis, Bremen (1991).
12. M. Kac, *Am. Math. Monthly* **73**, 1 (1966).
13. M. V. Berry, *Eur. J. Phys.* **2**:91 (1981).
14. E. P. Wigner, *Phys. Rev.* **40**:749 (1932).
15. M. V. Berry, Semiclassical mechanics of regular and irregular motion, in *Les Houches, Session XXXVI, Chaotic Behavior of Deterministic Systems* (North-Holland, Amsterdam, 1983).
16. M. V. Berry, *Proc. Soc. A* **287**:237 (1977).
17. M. C. Gutzwiller, *Chaos in Classical and Quantum Mechanics* (Springer-Verlag, New York, 1990).